Verlag

Georg Thieme Verlag KG
Rüdigerstraße 14
70469 Stuttgart
www.thieme.de/roefo
www.thieme-connect.de

Ex-Vivo Human Lung Tumor Model: Use for Temperature Measurements during Thermal Ablation of NSCLC

Humanes Ex-vivo-Lungentumormodell: Nutzung für Temperaturmessungen während der Thermoablation von NSCLC

Autoren F. Koch[1], A. Vietze[1], U. Laskowski[2], C. Ritter[3], A. Linder[4], N. Hosten[1]

Institute
[1] Diagnostic Radiology and Neuroradiology, Ernst-Moritz-Arndt-Universität Greifswald
[2] Thoracic Surgery, Märkische Kliniken Lüdenscheid
[3] Pharmacology, Ernst-Moritz-Arndt-Universität Greifswald
[4] Thoracic Surgery, Klinikum Bremen-Ost

Key words
- thorax
- ablation procedures
- interventional procedures

Zusammenfassung

Ziel: In dieser Studie wurde ein menschliches Ex-vivo-Lungenkrebsmodell verwendet, um die Temperaturentwicklung bei der Ablation mit 1 Laserfaser mit der Entwicklung beim Gebrauch von 2 Laserfasern zu vergleichen. Zudem wurde untersucht, ob die Temperaturdiffusion in normalem Lungengewebe von dem in Tumorgewebe abweicht.

Material und Methoden: 48 Lungenpräparate, die nichtkleinzellige Bronchialkarzinome enthielten, wurden mit dem Ventilations- und Perfusionsmodell verbunden und mit 1 (22 Präparate, Gruppe 1) oder, in einer zweiten Phase, mit 1 (13 Präparate, Gruppe 2) oder 2 Laserfasern (13 Präparate, Gruppe 3) behandelt. Während der Ablation des Tumors wurde die Temperatur alle 5 s interstitiell gemessen.

Ergebnisse: Eine Laserbehandlung und die Temperaturkontrolle war in allen Fällen technisch durchführbar. 30 min nach dem Beginn der Laserung mit 1 Faser wurde in 10 mm Entfernung von dieser eine Temperatur von 61 ± 17 °C in Gruppe 1 und von 74 ± 11 °C in Gruppe 2 erreicht (p = 0,1). In der Mitte zwischen 2 Laserfasern, die 20 mm voneinander entfernt waren, wurde eine Temperatur von 93 ± 7 °C erreicht. Nach 20-minütiger Ablation wurde in normalem Lungengewebe eine Temperatur von 77 ± 15 °C in 10 mm Entfernung erreicht.

Schlussfolgerung: Das Ex-vivo-Modell ermöglicht die Durchführung der laserinduzierten Thermotherapie an einer perfundierten und ventilierten Lunge. Der Einsatz einer zweiten Laserfaser erhöht die Temperatur signifikant (p < 0,05). Die Temperaturentwicklung in normaler Lunge unterscheidet sich nicht signifikant von der in Tumorgewebe (p = 0,24).

eingereicht 25.11.2009
akzeptiert 16.10.2010

Bibliografie
DOI http://dx.doi.org/10.1055/s-0029-1245884
Online-Publikation: 17.12.2010
Fortschr Röntgenstr 2011; 183: 251 – 259 © Georg Thieme Verlag KG Stuttgart · New York · ISSN 1438-9029

Korrespondenzadresse
Miss Franziska Koch
Diagnostic Radiology and Neuroradiology, Ernst-Moritz-Arndt-Universität Greifswald
Sauerbruchstraße
17487 Greifswald
Germany
Tel.: ++ 49/38 34/86 69 60
Fax: ++ 49/38 34/86 70 97
franzi_koch@hotmail.com

Abstract

Purpose: In the present study we used an ex-vivo human lung cancer model to compare temperature diffusion during thermal ablation using one laser fiber to that of a two-fiber approach. Furthermore, we examined whether there was a difference between temperature diffusion in normal lung tissue and tumor tissue during laser ablation.

Materials and Methods: 48 resected lung specimens containing non-small cell lung cancer were connected to a perfusion/ventilation apparatus and treated with 1 (22 specimens, group 1) or, in a second experiment, with 1 (13 specimens, group 2) or 2 (13 specimens, group 3) laser fibers. During tumor ablation, temperatures were measured interstitially every 5 sec. Laser ablation was followed by the taking of samples of 13 specimens for histological examination. For comparison we performed laser ablation in 7 specimens with normal lung tissue.

Results: Laser treatment and temperature control were technically feasible in all samples. Thirty min after starting laser ablation with 1 fiber, a temperature of 61 ± 17 °C was achieved in group 1 at a distance of 10 mm from the laser fiber and a temperature of 74 ± 11 °C was achieved in group 2 (p = 0.1). In the middle between two active laser fibers placed 20 mm apart, a temperature of 93 ± 7 °C was achieved. The temperature reached in normal lung tissue after 20 min of laser ablation was 77 ± 15 °C at a distance of 10 mm from the laser fiber.

Conclusion: The ex-vivo model allowed performance of laser-induced thermal ablation in the perfused and ventilated lung. The use of two laser fibers increases the achieved temperatures significantly (p < 0.05). Temperatures reached in normal lung tissue were as high as in tumor tissue (p = 0.24).

Table 1 Summary of the key data of the experiments including number of specimens, mean tumor diameter, mean temperature at probe a or c and mean slope at probe a or c.

Tab. 1 Zusammenfassung der Kerndaten der Experimente inklusive der Probenanzahl, des durchschnittlichen Tumordurchmessers, der mittleren Temperatur an Sonde a oder c und des gemittelten Temperaturanstiegs an Sonde a oder c.

group	number of specimens	mean tumor diameter	mean temperature at probe a or c (group 3)	mean slope at probe a or c (group 3)
1	22	4.86	59.3 °C	3.0 °C/min
2	13	4.03	59.0 °C	2.3 °C/min
3	13	4.58	78.7 °C	4.9 °C/min
4	4	4.5	63.8 °C	5.3 °C/min
5	3	7.5	50.1 °C	2.8 °C/min
6	7	5.6	58.3 °C	4.1 °C/min
7	7	normal lung	65.7 °C	4.6 °C/min

Introduction

Thermal ablation of lung tumors was first performed experimentally in the 1990s [1, 2]. Its clinical use started at the beginning of the 21st century [3–6]. Techniques have advanced considerably since then. Nevertheless, it is still difficult to estimate the adequacy of temperature induced in lung tumors during ablation. This is a problem in treating pulmonary tumors, whether laser or radiofrequency ablation is used, because of the specific properties of the tissues present in the lung (air-filled alveoli, vessels, tumor, etc.). There are several options for evaluating a new technique for cancer treatment, for example, animal models [2, 7], human ex-vivo preparations, and clinical trials. Tumors implanted in small animals do not adequately reflect the lesion sizes encountered in the clinical setting, which are crucial for the outcome of thermal ablation. Tumor models in large experimental animals are difficult to establish. Furthermore, tumor biology, e.g. in rabbit models, may differ from that in humans [8]. Tumor implantation may also lead to rapid tumor cell migration through the blood stream and lymphatic circulation [8].

To avoid problems associated with animal models, we used an ex-vivo model established in other research fields, the so-called isolated human lung perfusion model [9], to monitor temperature diffusion during laser ablation by direct invasive temperature measurement. The aim of this study was to assess temperature diffusion at predefined distances from one or two laser fibers during thermal ablation of non-small cell lung malignancies.

Materials and Methods

The standardized terminology published by Goldberg et al. is used [10].

The experiments were performed in the department of thoracic surgery at a center for lung disease (Hemer, Germany). This institution performs lung resections in 1,300 patients annually. Lung specimens from 48 patients with non-small cell lung cancer were used for the experiments (**Table 1**; **Fig. 1**). Between August 2004 and October 2007, 41 of these underwent lobectomy (85.4%), 3 bilobectomy (6.3%), and 4 pneumonectomy (8.3%). The resected tumors ranged in diameter from 1.0 cm to 12.0 cm with a mean of 4.5 cm.

Surgery was medically indicated in all patients. Our study was approved by the regional ethics committee. Written informed consent was obtained from all patients before their operation.

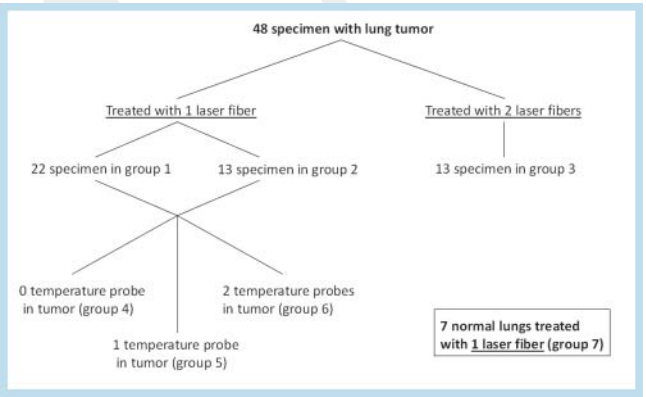

Fig. 1 Summary of the groups.

Abb. 1 Gruppenaufteilung.

Immediately after surgical removal, the lung specimens were brought into the laboratory. After a first gross examination and palpation of the tumor, cannulae were attached to the main arteries and bronchi (**Fig. 2**). The detailed design of the ex-vivo model was described by Linder et al. [9]. **Fig. 3** shows a diagram of the ex-vivo model.

Immediately, the ex-vivo model was filled with 1 to 1.5 liters of a buffered solution. This solution was prepared daily according to the following formulation (per liter of distilled water):

- 9.6 g Dulbecco's Phosphate Buffered Saline (Sigma-Aldrich Chemistry GmbH, P.O. 1120, 89552 Steinheim/Germany)
- 991.1 mg glucose
- 367.5 mg $CaCl2 \times 2\,H2O$.

After completion of these preparations, an adequately sized tissue sample was removed from the lung specimens, preserved in formalin, and then brought to the pathology department for final pathological classification of the tumor. Care was taken not to alter the circulation and ventilation properties of the specimens, which was a problem in some centrally located tumors. If major structures were damaged, the specimen was discarded (n = 1).

After connection of the lung specimen to the ventilation and perfusion apparatus, the respiratory parameters were adjusted. Initially, this was done exclusively on the basis of the gross impression of the specimen. The volume of the perfusate moved by the roller pumps was set high enough to avoid desiccation and low enough to prevent lung edema.

After 5 min of ventilation and perfusion, blood gas analysis was performed. According to the results, parameter settings of the

Fig. 2 Lung specimen in the ex-vivo model; 1 – two cannulae sutured to two main arteries, 2 – endotracheal tube sutured to the bronchus. Perfusate leaves the lung before it is collected in the container at the bottom and recirculated by the roller pumps (not shown).

Abb. 2 Lungenlappen im Ex-vivo-Modell; 1 – zwei Kanülen, die mit den 2 Hauptarterien verbunden sind, 2 – Tubus, der am Bronchus fixiert wurde. Das Perfusat verlässt die Lunge und wird anschließend im Auffangbehälter gesammelt, bevor es durch die Rollerpumpen (nicht abgebildet) rezirkuliert.

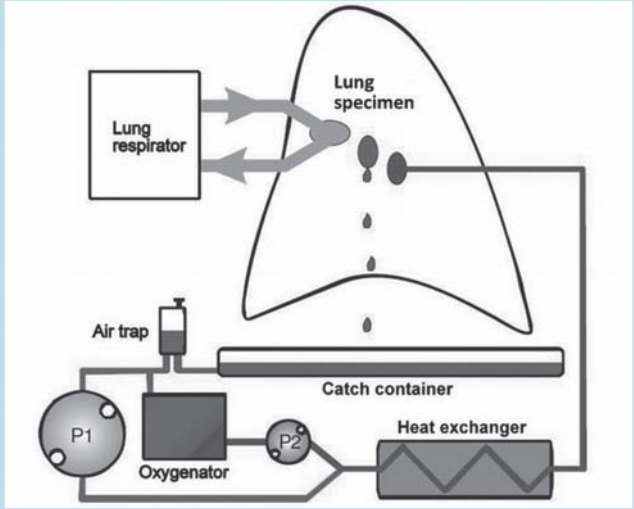

Fig. 3 Diagram of the ex-vivo model. The lung specimen is connected with a lung respirator and a system of roller pumps transporting heated perfusate to the main arteries. The perfusate leaves the specimen through the open veins and is collected for reintroduction into the circulation.

Abb. 3 Diagramm des Ex-vivo-Modells. Das Lungenpräparat wird mit dem Beatmungsgerät verbunden und ein System aus Rollerpumpen transportiert erwärmtes Perfusat zu den Hauptarterien. Das Perfusat verlässt das Präparat über die offen gelassenen Venen, wird aufgefangen und wieder der Zirkulation zugeführt.

ex-vivo model were readjusted. Especially the pH and pCO2 needed to be modified regularly. If pCO2 was below 35 mm Hg or the pH was over 7.6, carbon dioxide was introduced via the membrane oxygenator. If the pH was below 7.35, bicarbonate was added to the system. After correction another blood gas analysis was performed and then repeated every 30 min. The O_2 partial pressure was maintained between 80 and 120 mm Hg.

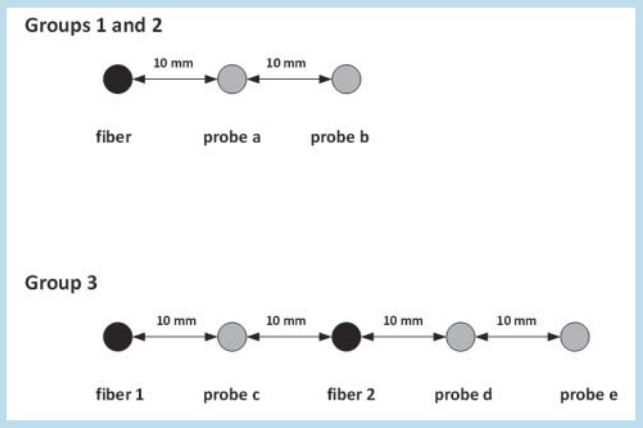

Fig. 4 **a** Arrangement of the laser fiber and the temperature probes in the experiments with 1 laser fiber. **b** Arrangement of the laser fibers and the temperature probes (c, d and e) in the experiments with two laser fibers.

Abb. 4 **a** Anordnung der Laserfaser und der Temperatursonden in den Experimenten mit 1 Laserfaser. **b** Anordnung der Laserfasern und der Temperatursonden in den Experimenten mit 2 Laserfasern.

After establishing a stable, near-physiological setting in the system, the laser applicator(s) and the temperature probes were positioned in the tumor or the surrounding lung tissue. We used a distally open 5.5-French miniaturized laser applicator (Monocath®, Trumpf, Umkirch/Germany) consisting of a 5.5-French Teflon cannula as the main part. The procedure began by inserting a titanium mandrin into the Teflon cannula to position one or two laser applicators in each tumor. The tumors were palpated and the laser applicator(s) inserted manually. Positioning of the applicator(s) was followed by placement of the temperature probes (Thermocouples, B+B Thermotechnology, Donaueschingen/Germany and a Digital 4-Channel Data Logger 309/K204, Conrad Electronic, Hirschau/Germany). The positions of fiber(s) and temperature probes are shown in ▶ **Fig. 4**. We used a plastic spacer to assure a reproducible distance of 10 mm between the laser fiber and each temperature probe.

After manual control to ensure correct positioning, the titanium mandarin was replaced by the laser fiber, which was connected to a neodymium:yttrium-aluminium-garnet laser (Nd:YAG, Trumpf TT YAG 80, Trumpf, Umkirch/Germany) with a wavelength of 1064 nm, which we also use in the clinical setting. Before inserting the fiber into the Teflon cannula, it was tested by checking the pilot light. The laser fiber had a diffusor tip with a length of 2.5 cm and a diameter of 0.9 mm (Microdome®, Trumpf, Umkirch/Germany).

Additionally, the laser applicator had an access point for an infusion line for cooling of the fiber. Cooling was accomplished using 0.9% sodium chloride supplied by a perfusion pump with a flow of 80 ml per hour.

If two laser fibers were used, a two-way beam splitter (Typ TT SWITCH 2, Trumpf Medicine Systems GmbH+Co. KG, Umkirch/Germany) was interposed between the laser and the fibers. In a first stage of the experiments, which included 22 specimens (▶ **Fig. 1**), only one laser fiber was used. Analysis of the results of this pilot phase revealed an unsatisfying temperature diffusion. To determine whether a second laser fiber would improve temperature diffusion a second stage followed. The hypothesis was that simultaneous use of two fibers would induce a higher temperature. Therefore, in a second stage in-

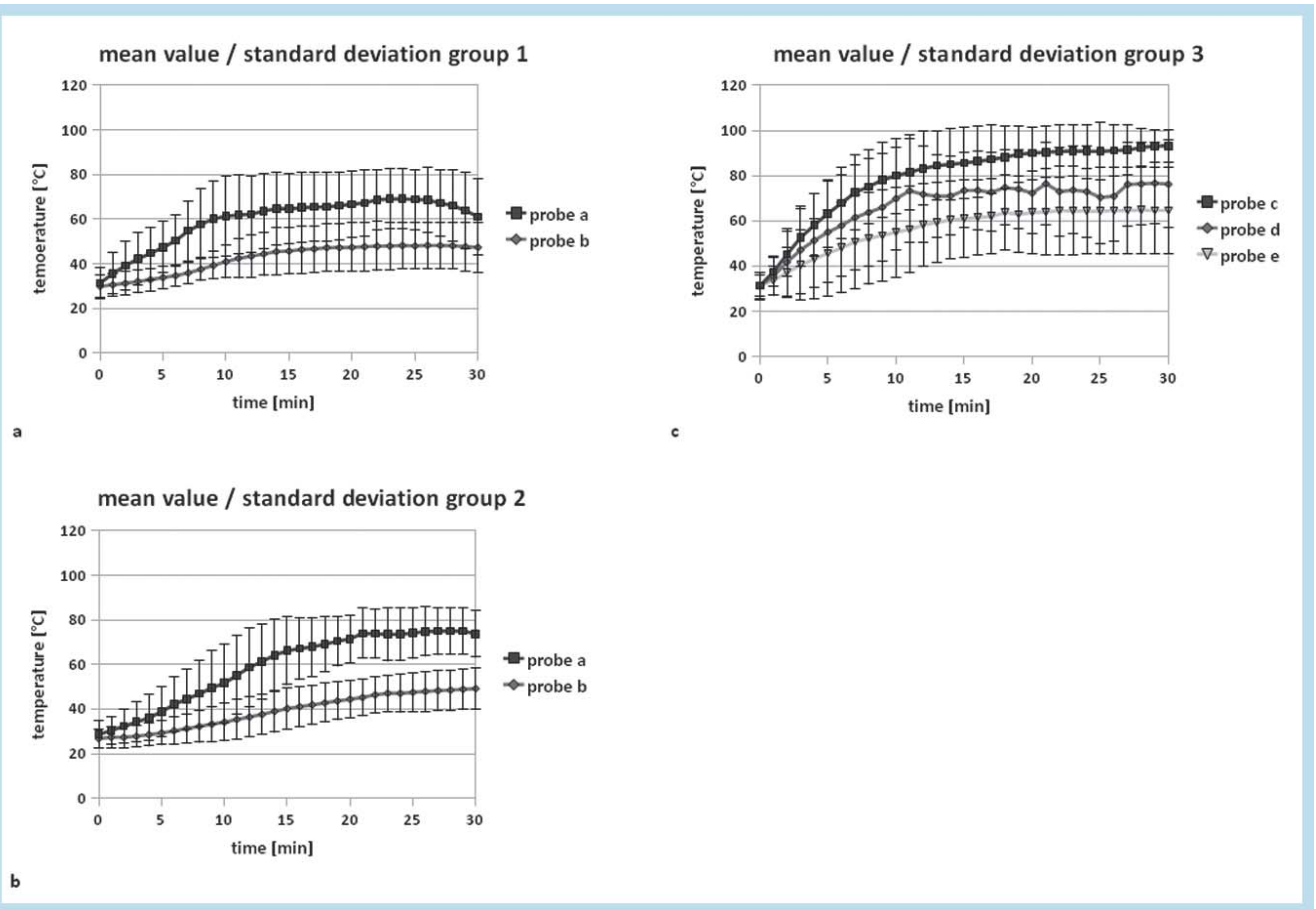

Fig. 5 Mean temperatures and standard deviations measured at temperature probes a and b/probes c, d and e during the experiments of group 1 **(a)**, group 2 **(b)** and group 3 **(c)**; time in minutes is plotted against the x-axis and temperature in °C against the y-axis.

Abb. 5 Durchschnittstemperatur und Standardabweichung an den Temperatursonden a und b bzw. c, d und e während der Gruppe-1- **(a)**, Gruppe-2- **(b)** und Gruppe-3-Experimente **(c)**; die Zeit in Minuten ist auf der x-Achse aufgetragen und die Temperatur in °C auf der y-Achse.

cluding 26 specimens, one group was treated using one laser fiber and a second group using two laser fibers (n = 13 each). The specimens were consecutively treated alternating between the one-fiber and two-fiber approach regardless of any attributes of the tumors or resected portions of the lung.

Laser application started with 8 watt output per fiber and was increased about 2 watts per fiber every minute until reaching either the target temperature of 60 °C or 20 watts. The target temperature of 60 °C was not chosen with the intention of ablating the tumor completely. It was rather a question of continuous temperature diffusion without high risk of carbonization. The energy necessary to achieve at least 60 °C was then kept constant for 20 min regardless of further temperature development. During laser application, temperature was measured every 5 sec.

After the end of laser ablation, the specimens were cut along the insertion direction of the laser fiber. That allowed us to evaluate the correct position of the temperature probes retrospectively. We did not have to exclude any specimens because of incorrectly positioned temperature probes. This procedure seemed to be more useful than ultrasound because ultrasound would not be feasible in the air-filled lung.

In addition, we took samples from 14 specimens in group 1 and 2 to assess by histological examination how many temperature probes were positioned in the tumor (group 4: no probe; group 5: one probe; group 6: two probes; ▶ **Fig. 1**). To correlate different temperature diffusion with different tissues, we additionally performed 7 laser ablations with one fiber in normal lungs (group 7). These laser ablations followed the same laser protocol as described above. The only difference was that laser ablation was terminated 10 min after reaching 60 °C because the main point of interest was more on the slope than on the maximum temperature. The reason for the main interest being the slope and not the maximum temperature was that the focus of this paper was factors influencing temperature diffusion, not clinical use.

All measured data are presented as mean ± standard deviation. The slope of the temperature curves was calculated using the following formula:

$$m = \frac{\Delta y}{\Delta x} = \frac{y_2 - y_1}{x_2 - x_1}.$$

ΔX approximates the differences in x-values, which in this case were differences in time values ($x_2 = 10$ min and $x_1 = 0$ min).

ΔY approximates the differences in y-values, which in this case were differences in temperature values at minute 0 and minute 10.

The unit of m is °C/min.

Nonparametric statistic evaluation (Wilcoxon test) was performed using common statistical software (SPSS).

Results

Results with one laser fiber (group 1)

22 lung specimens were treated with 1 laser fiber in group 1 (**Table 1**). There were 12 adenocarcinomas (54.6%), 7 squamous cell carcinomas (31.8.9%), 2 atypical carcinoids (9.1%), and 1 bronchoalveolar carcinoma (4.5%).

Temperature diffusion at a distance of 10 mm from the laser fiber (probe a) showed an asymptotic trend when approaching 70 °C (**Fig. 5a**). The increasing wattage applied in the initial phase of thermoablation produced a steep increase in temperature. Then, at 65 °C, the curve flattened noticeably and plateaued at 70 °C before slowly decreasing during the last five min.

The end temperature reached after 30 min of laser ablation was 61 ± 17 °C. The overall average temperature during laser application was 59 ± 14 °C. The target temperature of 60 °C was reached after 9 min in most experiments. The slope of the curve between minute 0 and minute 10 was 3.0 °C/min.

The temperature diffusion at a distance of 20 mm from the laser fiber (probe b; **Fig. 5a**) was also asymptotic. The asymptote, however, was reached at a much lower temperature of 50 °C. After 30 min of laser ablation, it decreased to 47 ± 11 °C. The overall average temperature during laser application was 42 ± 9 °C. A temperature of at least 60 °C was only reached in 3 of 22 laser ablations (13.6%). The slope of the curve between minute 0 and minute 10 was 1.1 °C/min.

Results with one laser fiber (group 2)

Thirteen lung specimens were treated with 1 laser fiber in group 2 (**Table 1**). There were 2 adenocarcinomas (15.4%), 9 squamous cell carcinomas (69.2%), 1 bronchoalveolar carcinoma (7.7%) and 1 large-call undifferentiated carcinoma (7.7%).

Temperature diffusion at both distances from the laser fiber showed an asymptotic trend as well (**Fig. 5b**)

The end temperature reached after 30 min of laser ablation was 74 ± 11 °C at probe a (10 mm from the laser fiber). The overall average temperature during laser application was 59 ± 12 °C. The target temperature of 60 °C was reached after 13 min in most experiments. The slope of the curve between minute 0 and minute 10 was 2.3 °C/min.

After 30 min of laser ablation, the temperature was 49 ± 9 °C at probe b (20 mm from the laser fiber). The overall average temperature during laser application was 40 ± 8 °C. A temperature of at least 60 °C was only reached in 1 of 13 laser ablations (7.7%). The slope of the curve between minute 0 and minute 10 was 0.7 °C/min.

Results with two laser fibers (group 3)

Thirteen lung specimens were treated with 2 laser fibers (**Table 1**). 6 tumors were classified as squamous cell carcinoma (46.2%), 5 as adenocarcinoma (38.5%), and 2 as large-cell undifferentiated carcinoma (15.3%).

Temperature probe c was positioned halfway between two laser fibers at a distance of 10 mm from both. The end temperature reached after 30 min of laser ablation was 93 ± 7 °C (**Fig. 5c**). The overall average temperature during laser application was 79 ± 13 °C. The target temperature of 60 °C was reached after 5 min in most experiments. The slope of the curve between minute 0 and minute 10 was 4.9 °C/min. In all 13 experiments (100%), a temperature of at least 60 °C was achieved.

The temperature measured at a distance of 10 mm from one fiber and 30 mm from the second (probe d; **Fig. 5c**) increased asymptotically to 76 ± 19 °C after 30 min of laser ablation. The target temperature was reached after a mean of 7 min. Overall, a mean temperature of 66 ± 19 °C was obtained. In 10 of 13 experiments (76.9%), a temperature of at least 60 °C was achieved. The slope of the curve between minute 0 and minute 10 was 3.8 °C/min.

Lower temperatures were reached at a distance of 20 mm from one and 40 mm from the second fiber (probe e; **Fig. 5c**). The temperature peaked at 65 ± 19 °C after 30 min of laser ablation. Overall, a mean temperature of 59 ± 18 °C was obtained. At this distance, a temperature of at least 60 °C was reached after a mean of 14 min, and was not reached at all in only 3 cases (23.1%). The slope of the curve between minute 0 and minute 10 was 2.4 °C/min.

Results of the group with no temperature probe in the tumor (group 4)

This group included 4 specimens (**Table 1**). 3 of them were classified as adenocarcinoma (75%) and 1 as atypical carcinoma (25%). The end temperature reached after 20 min of laser ablation was 79 ± 6 °C at probe a (10 mm from the laser fiber; **Fig. 6a**). The overall average temperature during laser application was 64 ± 9 °C. The slope of the curve between minute 0 and minute 10 was 5.3 °C/min.

After 20 min of laser ablation, the temperature was 49 ± 13 °C at probe b (20 mm from the laser fiber). The overall average temperature during laser application at this distance was 40 ± 8 °C. The slope of the curve between minute 0 and minute 10 was 1.9 °C/min.

Results of the group with one temperature probe in the tumor (group 5)

This group included 3 specimens (**Table 1**). 2 of them were classified as adenocarcinoma (67%) and 1 as squamous cell carcinoma (33%). The end temperature reached after 20 min of laser ablation was 56 ± 17 °C at probe a (10 mm from the laser fiber; **Fig. 6b**). The overall average temperature during laser application was 50 ± 15 °C at this distance. The slope of the curve between minute 0 and minute 10 was 2.8 °C/min.

After 20 min of laser ablation, the temperature at probe b (20 mm from the laser fiber) was 35 ± 13 °C. The overall average temperature during laser application was 39 ± 7 °C. The slope of the curve between minute 0 and minute 10 was 0.9 °C/min.

Results of the group with two temperature probes in the tumor (group 6)

This group included 7 specimens (**Table 1**). 3 of them were classified as squamous cell carcinoma (42.8%), 2 as adenocarcinoma (28.6%), 1 as bronchoalveolar carcinoma (14.3%) und 1 as large undifferentiated carcinoma (14.3%).

The end temperature reached after 20 min of laser ablation at probe a (10 mm from the laser fiber) was 72 ± 14 °C (**Fig. 6c**). The overall average temperature during laser application was 58 ± 13 °C. The slope of the curve between minute 0 and minute 10 was 4.1 °C/min.

After 20 min of laser ablation, the temperature at probe b (20 mm from the laser fiber) was 47 ± 7 °C. The overall average temperature during laser application was 36 ± 5 °C. The slope of the curve between minute 0 and minute 10 was 1.1 °C/min.

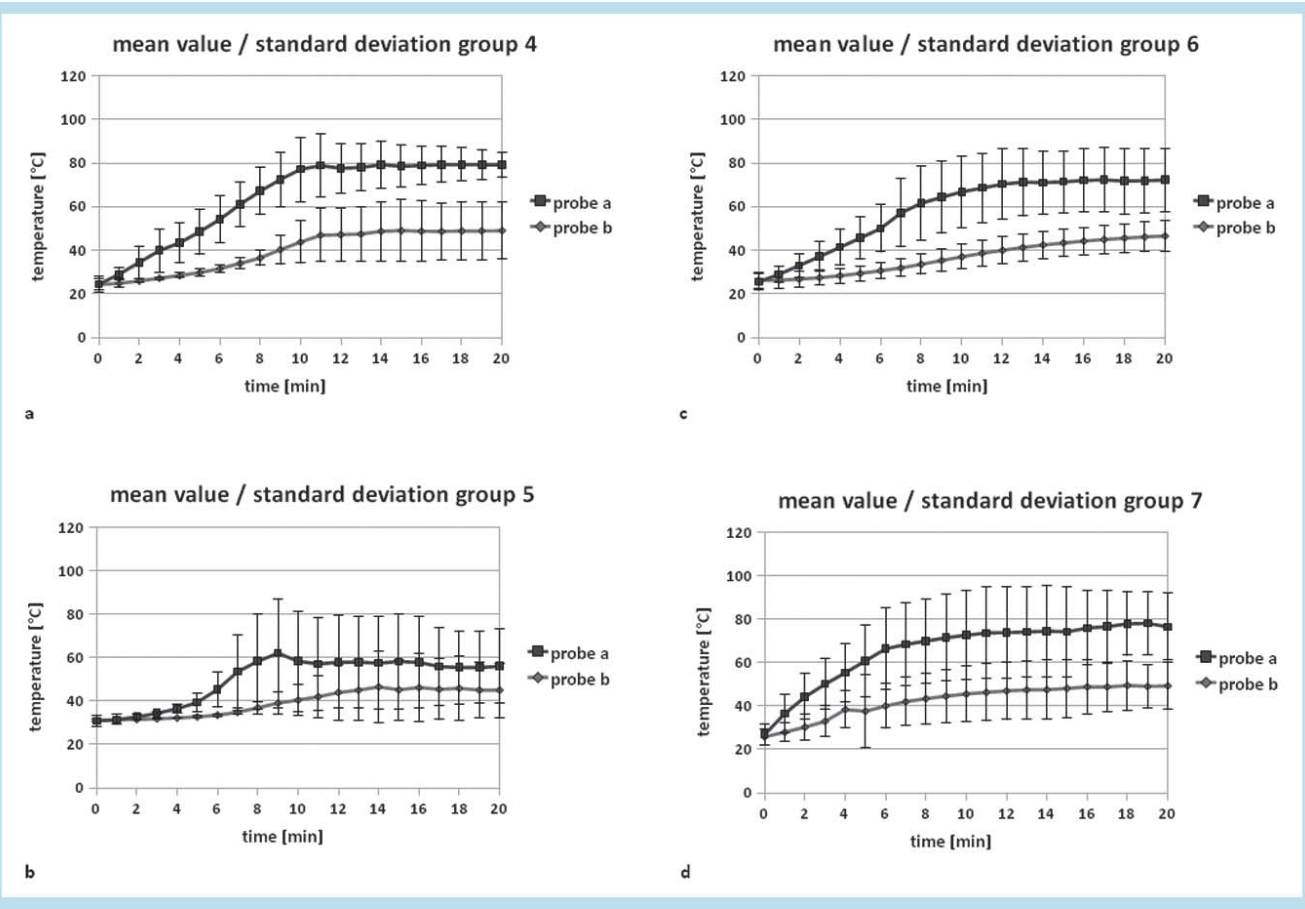

Fig. 6 Mean temperatures and standard deviations measured at temperature probes a and b during the experiments of group 4 **(a)**, group 5 **(b)**, group 6 **(c)** and group 7 **(d)**; time in minutes is plotted against the x-axis and temperature in °C against the y-axis.

Abb. 6 Durchschnittstemperatur und Standardabweichung an den Temperatursonden a und b während der Gruppe-4- **(a)**, Gruppe-5- **(b)**, Gruppe-6- **(c)** und Gruppe-7-Experimente **(d)**; die Zeit in Minuten ist auf der x-Achse aufgetragen und die Temperatur in °C auf der y-Achse.

Results in a normal lung (group 7)

This group included 7 specimens (**Table 1**).

Temperature diffusion at a distance of 10 mm from the laser fiber (probe a) showed an asymptotic trend when approaching 75 °C (**Fig. 6 d**). The end temperature reached after 20 min of laser ablation was 77 ± 15 °C. The overall average temperature during laser application was 66 ± 17 °C. The slope of the curve between minute 0 and minute 10 was 4.6 °C/min.

The temperature development at a distance of 20 mm from the laser fiber (probe b) was also asymptotic. The asymptote, however, was reached at a much lower temperature of 50 °C. After 20 min of laser ablation, it decreased to 49 ± 11 °C. The overall average temperature during laser application was 41 ± 11 °C. The slope of the curve between minute 0 and minute 10 was 2.0 °C/min.

Discussion

Lung cancer causes nearly one third (28.6%) of all cancer-related deaths [11]. Surgery with curative intent, which may prolong survival, is still the gold standard of therapy. However, this therapeutic option is only available for patients with limited disease (stages I and II). Lung cancer rarely causes early symptoms, which is why only one third of patients have stage I or II disease at the time of diagnosis. Chemotherapy and radiotherapy are available for patients with more advanced lung cancer. In these cases treatment is often palliative. Consequently, the 5-year survival rate is only 3.5% in stage V patients compared to 52.6% in stage I patients [11].

In view of this situation, there is an ongoing search for alternative treatment options, especially for patients who are inoperable either because of their poor condition or their advanced tumor stage. Possible options to improve survival in inoperable patients are minimally invasive thermo-ablative techniques. Radiofrequency ablation and laser-induced thermal ablation have been used in lung cancer as these methods have already proved their clinical importance in the therapy of primary and secondary liver tumors [12 – 14]. However, on-line monitoring of these treatments in the lung is still limited to indirect morphological findings in computed tomography, like ground glass opacity [15, 16]. Obviously, on-line thermometry using MRI, which has made some advances in the monitoring of liver tumor ablation [17, 18], is not possible in the lung. Therefore, a model coming close to the clinical situation encountered in the thermal ablation of tumor patients is all the more desirable.

Animal models have been used by some groups, with the problems commonly encountered being described by Lee et al. [19]. The group performed radiofrequency ablation in an

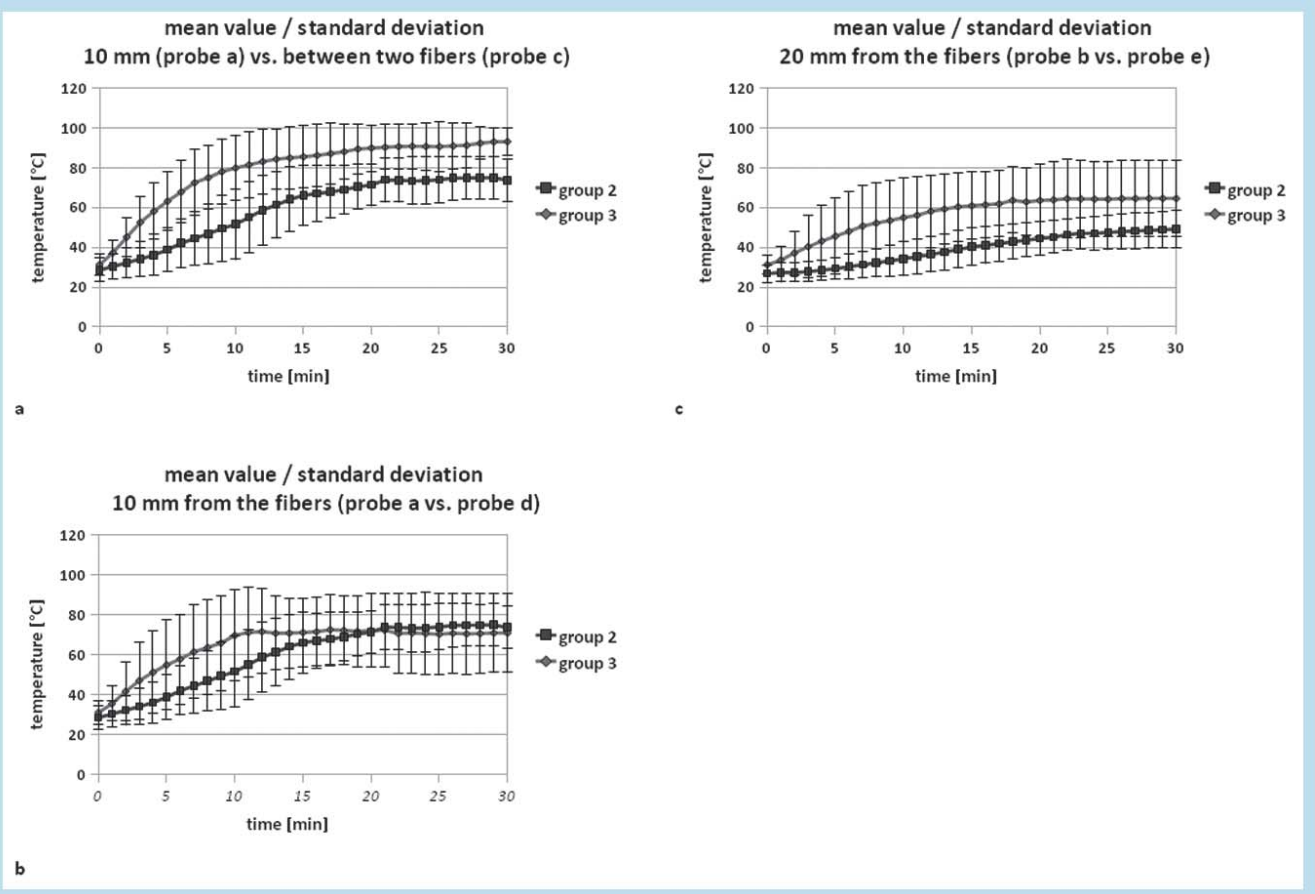

Fig. 7 Comparison of the temperature diffusion of group 2 and group 3; time in minutes is plotted against the x-axis and temperature in °C against the y-axis. The temperature difference was significant at probe a vs. c **(a)** and at probe b vs. e **(c)** ($p < 0.05$). The comparison of the temperature diffusion at probe a and d **(b)** was not statistically significant ($p = 0.51$).

Abb. 7 Vergleich der Temperaturentwicklungen von Gruppe 2 und 3; die Zeit in Minuten ist auf der x-Achse aufgetragen und die Temperatur in °C auf der y-Achse. Der hier gezeigte Temperaturunterschied von Sonde a vs. Sonde c **(a)** und Sonde b vs. Sonde e **(c)** ist signifikant ($p < 0{,}05$). Der Vergleich von Sonde a und d **(b)** ist hingegen nicht signifikant ($p = 0{,}51$).

in-vivo rabbit lung model and in an ex-vivo bovine lung model. These experiments had to be performed on normal lung tissue, limiting the amount of information generated for optimizing thermal ablation of lung tumor tissue. Secondly, the ex-vivo experiments were performed using a bovine lung that was not perfused and only once distended by the insufflation of room air. The cooling effects of perfusion, being well known to influence thermal ablation ("heat sink effect"), could not be simulated in these animal models. Thirdly, the authors report that rabbit lung did not have enough volume to use the same protocol as when treating patients. As a result, treatment was shorter and less energy was applied, which is why the results are not directly applicable to the clinical setting.

A human ex-vivo model appears to be well suited to test and optimize thermal ablation. It may be employed after experiments in explanted animal organs and before treating patients. The ex-vivo model [9] we present here allowed direct invasive temperature measurement using an inexpensive and readily available technique. Such measurements are not possible in patients.

Nevertheless, there are also limitations to this ex-vivo model. The most obvious one is that we only achieved near-physiological settings. However, there is a window of 6 to 8 hours during which the condition of the lung is not altered to any significant extent by these near-physiological conditions. We therefore think that the model is suitable to analyze several parameters of thermoablation and improve protocols for ablation treatment.

Our temperature measurements show that, when two laser fibers are used simultaneously, a summation effect is achieved in the center between both fibers (**Fig. 7**). The highest temperatures were measured by the temperature probe positioned exactly midway between two laser fibers. The difference with respect to the temperature at a probe 10 mm from one fiber was significant (**Fig. 7a**; $p < 0.05$). At a distance of 10 mm from one laser fiber, the slope showed obvious differences, but the maximum temperature was not significantly increased when a second fiber was positioned at a distance of 30 mm (**Fig. 7b**). For clinical practice these observations suggest that it is best to place several applicators at the periphery of a larger tumor. However, the repositioning of applicators may increase the risk of tumor seeding [20–21].

At a distance of 20 mm from the laser fiber, significant differences between the one-fiber and the two-fiber groups became apparent (**Fig. 7c**; $p < 0.05$). The experiments with two laser fibers resulted in 77 of the experiments in a temperature of at least 60 °C, whereas experiments with one laser fiber did not reproducibly reach this temperature.

The calculation of slopes between minute 0 and minute 10 revealed differences between the experiments with 1 fiber and

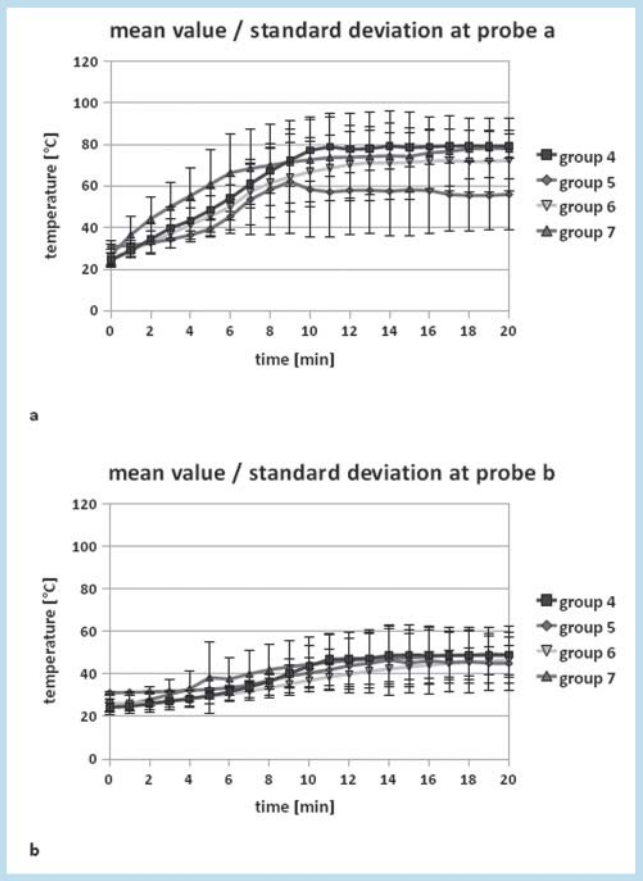

Fig. 8 Comparison of the temperature diffusion of group 4 – 7 (**a** probe a; **b** probe b); time in minutes is plotted against the x-axis and temperature in °C against the y-axis. None of these comparisons were statistically significant.

Abb. 8 Vergleich der Temperaturentwicklungen der Gruppen 4 – 7 (**a** Sonde a; **b** Sonde b); die Zeit in Minuten ist auf der x-Achse aufgetragen und die Temperatur in °C auf der y-Achse.

those with 2 fibers. When using one fiber, flatter slopes were calculated for the temperature increase (3.0 °C/min and 2.3 °C/min at probe a and 1.1 °C/min and 0.7 °C/min at probe b) than when using 2 fibers simultaneously (4.9 °C/min at probe c, 3.8 °C/min at probe d and 2.4 °C/min at probe e).

The results of the second part of the experiments imply that there is no statistically significant difference between temperature diffusion in normal lung tissue and tumor tissue (**Fig. 8**). This conclusion is probably limited by the fact that there were only a few samples in each group. At a distance of 10 mm, the averaged temperature after 20 min was 72 ± 14 °C (tumor; group 6) vs. 77 ± 15 °C (normal lung; group 7; p = 0,24) and at a distance of 20 mm, it was 47 ± 7 °C (tumor; group 6) vs. 49 ± 11 °C (normal lung; group 7; p = 0,18). A distance of maximal 20 mm is probably too short for the supposed isolating effect of normal lung tissue [22].

Notwithstanding the above results, recent reviews still make surgery the therapy of choice for lung cancer patients with limited disease stages [23 – 25]. However, even these reviews underline the increasing impact of thermoablation techniques. They demand randomized controlled studies to define the role of thermoablation techniques alone and in conjunction with other therapeutic approaches such as cisplatin-based chemotherapy. The ex-vivo model we used is well suited to evaluate one aspect of thermoablation, namely use of one fiber alone versus two fibers simultaneously. Direct on-line measurement of temperature made a precise comparison including end point and slope possible. Such data are difficult or impossible to obtain when treating patients. The use of human tissue and, especially, of tissue actually containing a tumor makes these experiments possibly more realistic than the use of animals [2, 7, 8]. Even if temperature is not as reliable as the extent of coagulation for the prediction of a successful ablation, coagulation occurs only at temperatures over 60 °C [26, 27]. Therefore, basic knowledge of temperature diffusion helps to increase the effectiveness of clinically used thermoablation.

References

1 *Goldberg SN, Gazelle GS, Compton CC et al.* Radiofrequency tissue ablation in the rabbit lung: efficacy and complications. Acad Radiol 1995; 2: 776–784
2 *Goldberg SH, Gazelle GS, Comptom CC et al.* Radio-frequency tissue ablation of VX2 tumor nodules in rabbit lung. Acad Radiol 1996; 3: 929–935
3 *Dupuy DE, Zagoria RJ, Akerley W et al.* Percutaneous radiofrequency ablation of malignancies in the lung. AJR 2000; 174: 57–59
4 *Suh R, Wallace A, Sheehan R et al.* Unresectable pulmonary malignancies: CT-guided percutaneous radiofrequency ablation – preliminary results. Radiology 2003; 229: 821–829
5 *Lee JM, Jin GY, Goldberg SN et al.* Percutaneous radiofrequency ablation for inoperable non-small cell lung cancer and metastases: preliminary report. Radiology 2004; 230: 125–134
6 *Hosten N, Stier A, Weigel C et al.* Laser-induced thermotherapy (LITT) of lung metastases: description of a miniaturized applicator, optimization, and initial treatment of patients. Fortschr Röntgenstr 2003; 175: 393–400
7 *Morrison PR, van Sonnenberg E, Shankar S et al.* Radiofrequency ablation of thoracic lesions: part 1, experiments in the normal porcine thorax. AJR 2005; 184: 375–380
8 *Wacker FK, Nour SG, Eisenberg R et al.* MRI-guided radiofrequency thermal ablation of normal lung tissue: in vivo study in a rabbit model. AJR 2004; 183: 599–603
9 *Linder A, Friedel G, Fritz P et al.* The ex-vivo isolated, perfused human lung model: description and potential applications. Thorac Cardiovasc Surg 1996; 44: 140–146
10 *Goldberg SN, Grassi CJ, Cardella JF et al.* Image-guided tumor ablation: standardization of terminology and reporting criteria. Radiology 2005; 235: 728–739
11 *Horner MJ, Ries LAG, Krapcho M. et al.* SEER Cancer Statistics Review, 1975 – 2006, National Cancer Institute. Bethesda, MDhttp://seer.cancer.gov/csr/1975_2006/ based on November 2008 SEER data submission, posted to the SEER web site, last visited: 22.6.2009
12 *Vogl TJ, Straub R, Eichler K et al.* Malignant liver tumors treated with MR imaging-guided laser-induced thermotherapy: experience with complications in 899 Patients (2,520 lesions). Radiology 2002; 225: 367–377
13 *Eickmeyer F, Schwarzmaier HJ, Müller FP et al.* Survival after laser-induced interstitial thermotherapy of colorectal liver metastases – a comparison of first clinical experiences with current therapy results. Fortschr Röntgenstr 2008; 180: 35–41
14 *Bruners P, Schmitz-Rode T, Günther RW et al.* Multipolar hepatic radiofrequency ablation using up to six applicators: preliminary results. Fortschr Röntgenstr 2008; 180: 216–22
15 *Clasen S, Krober SM, Kosan B et al.* Pathomorphologic Evaluation of Pulmonary Radiofrequency Ablation: Proof of Cell Death Is Characterized by DNA Fragmentation and Apoptotic Bodies. Cancer 2008; 113: 3121–3129
16 *Yamamoto A, Nakamura K, Matsuoka T et al.* Radiofrequency Ablation in a Porcine Lung Model: Correlation Between CT and Histopathologic Findings. AJR 2005; 185: 1299–1306
17 *Cernicanu A, Lepetit-Coiffé M, Viallon M et al.* New horizons in MR-controlled and monitored radiofrequency ablation of liver tumours. Cancer Imaging 2007; 7: 160–166
18 *Kühn JP, Puls R, Wallaschowski H et al.* Characteristics of necrosis after laser-induced thermotherapy in contrast-enhanced MRI and implications for treatment success. Fortschr Röntgenstr 2008; 180: 816–820

19 *Lee JM, Youk JH, Kim YK et al.* Radio-frequency thermal ablation with hypertonic saline solution injection of the lung: ex vivo and in vivo feasibility studies. Eur Radiology 2003; 13: 2540–2547
20 *Liu SYW, Lee KF, Lai PBS.* Needle track seeding: a real hazard after percutaneous radiofrequency ablation for colorectal liver tumors. World J Gastroenterol 2009; 15: 1653–1655
21 *Imamura J, Tateishi R, Shiina S et al.* Neoplastic seeding after radiofrequency ablation for hepatocellular carcinoma. Am J Gastroenterol 2008; 103: 3057–3062
22 *Ahmed M, Liu Z, Afzal KM et al.* Radiofrequency Ablation: effect of surrounding tissue composition on coagulation necrosis in a canine tumor model. Radiology 2004; 230: 761–767
23 *Haasbeek CJA, Senan S, Smit EF et al.* Critical review of non-surgical treatment options for stage I non-small cell lung cancer. The Oncologist 2008; 13: 309–319
24 *Zhu JC, Yan TD, Morris DL.* A systematic review of RFA for lung tumors. Annals of Surgical Oncology 2008; 15: 1765–1774
25 *Gillams A.* Lung tumor ablation – where are we now. Cancer Imaging 2008; 8: 116–117
26 *Germer CT, Isbert C, Roggan A et al.* Experimentelle Grundlagen der LITT – Energie und Temperaturfindung zur vollständigen Ablation experimenteller Lebertumoren und potenzielle Ursachen einer Tumorrezidiventstehung. In Vogl TJ, Mack MG, Balzer JO. Lebermetastasen, Diagnose – Intervention – Therapie. Berlin, Heidelberg, New York: Springer, 2001: 221–235
27 *Goldberg SN, Gazelle GS, Compton CC et al.* Treatment of intrahepatic malignancy with radiofrequency ablation: radiologic-pathologic correlation. Cancer 2000; 88: 2452–2463